Plasmon energy shift in mesoporous and double length-scale ordered nanoporous silica

J. S. Yin and Z. L. Wang[a)]
School of Materials Science and Engineering, Georgia Institute of Technology, Atlanta, Georgia 30332-0245

(Received 8 January 1999; accepted for publication 5 March 1999)

Electron energy-loss spectroscopy studies are reported on three different types of structures: solid silica spheres, mesoporous silica, and the double length-scale ordered (DLSO) porous silica. The mesoporous silica has porosity at the length scale of nanometers. The DLSO porous silica has an additional ordering on submicron hollows created by the template polystyrene spheres. The plasmon energy of the porous silica shows a significant shift in comparison to that of the bulk, suggesting that the local density of the bound electrons in the porous structures is lower than that in the bulk. This gives the possibility of tuning the electronic structure of silica by varying its porosity, leading to even lower dielectric loss. © *1999 American Institute of Physics.* [S0003-6951(99)02918-6]

Ordered self-assembly of hollow structures of silica,[1] carbon,[2] and titania[3,4] has drawn much attention recently because of their applications in low-loss dielectrics, catalysis, filtering, and photonics.[5] The structure is ordered on the length scale of the template spheres and the pore sizes are in submicron to micron range. Alternatively, ordered porous silica with much smaller pore sizes in nanosize range (<30 nm), produced deliberately by introducing surfactant, has also been processed,[6,7] in which the porosity is created by surfactants. This is the so-called mesoporous structure.

We have combined the two types of porosity into a new silica structure that has ordering and porosity on two length scales, one is at the scale of hollow spheres created by a template of polystyrene (PS) spheres, and the other is the nanocavities created by self-assembled molecular copolymers. This is the double length-scale ordered (DLSO) porous silica to be presented below. In this letter, we first describe the synthesis technique and the microstructure of the DLSO porous silica. Then the plasmon excitations in the mesoporous and DLSO porous materials will be studied to reveal the change in electronic structure as a result of introducing porosity.

The DLSO silica structure is synthesized by a simple chemical approach and is stable to temperatures as high as 500 °C. The processing of DLSO porous silica includes three steps. First, the ordered template of PS was created. A 15 wt. % water solution of the as-received PS (from Duke Scientific), with mean particle size of 203 nm and a standard deviation of 2.1%, was used as the raw material. Typically 40 ml solution was put in a perpendicular open-end glass tube with inner diameter of 1.5 mm and the drying process in air took about 10 h, forming the ordered template of PS. Second, after the template was dried, the silica precursor, tetraethoxysiliane (TEOS), and a surfactant copolymer $\{HO(CH_2CH_2O)_{106}[CH_2CH(CH_3)O]_{70}(CH_2CH_2O)_{20}H$, from BASF$\}$[7] was infiltrated into the space between the PS spheres in the ordered template. Finally, after the precursor was dried slowly at room temperature, heating of the template at 450 °C for 5 h resulted in the simultaneous formation of the ordered porosity at double length scales.

Figure 1(a) gives a transmission electron microscopy (TEM) image, recorded at 100 kV using a JEOL 100C, of the as-prepared silica porous material, clearly exhibiting ordering in the template spherical hollow scale. The size of the hollow spheres is 120 ± 8 nm, smaller than the size of the PS due to volume shrinkage. TEM images and diffraction patterns have shown that the packing of the hollow spheres have the hexagonal-close-packed (hcp) ($a_h=120\pm8$ nm) and the face-centered cubic (fcc) ($a_c=175\pm10$ nm) structures, and the silica is amorphous. The nanocavities formed in the walls of the shells are also revealed by the image, and their sizes are 4–5 nm and the interpore distance is 8 ± 0.5 nm. The Fourier transform of the image [Fig. 1(b)] shows the ordering at both length scales, and the structure is schematically illustrated in Fig. 1(c).

The porous material can be made into macroscopic sizes and the ordered structure is still preserved. Large area and large quantity of the specimen can be made using the technique and the order preserves to a size as large as ~100 μm or more [Fig. 2(a)]. Scanning electron microscopy (SEM) image shows that the hollow spheres are interconnected due to the contacted close packing of the template PS spheres [Fig. 2(b)]. Thus, gases or liquids can be filtrated into the substrate,[8] suitable for applications in filtering. The larger wall thickness presented in the SEM image is likely due to the surface coating layer to reduce the charging and the limited image resolution (~10 nm at 5 kV).

To reveal the change in intrinsic electronic structure of the silica as a result of creating high porosity, electron energy-loss spectroscopy (EELS) has been applied to examine the energy shift in the plasmon band. The solid silica spheres were processed by hydrolysis of TEOS [Fig. 3(b)].[9] The mesoporous silica was processed by the same procedure except no PS sphere template [Fig. 3(c)].[7] The EELS experiments were carried out at 200 kV using a Hitachi HF-2000 TEM and the energy resolution of the system was ~1 eV. EELS spectra were acquired at an energy dispersion of 0.3 eV per channel, and the plasmon energy is calibrated in ref-

a)Electronic mail: zhong.wang@mse.gatech.edu

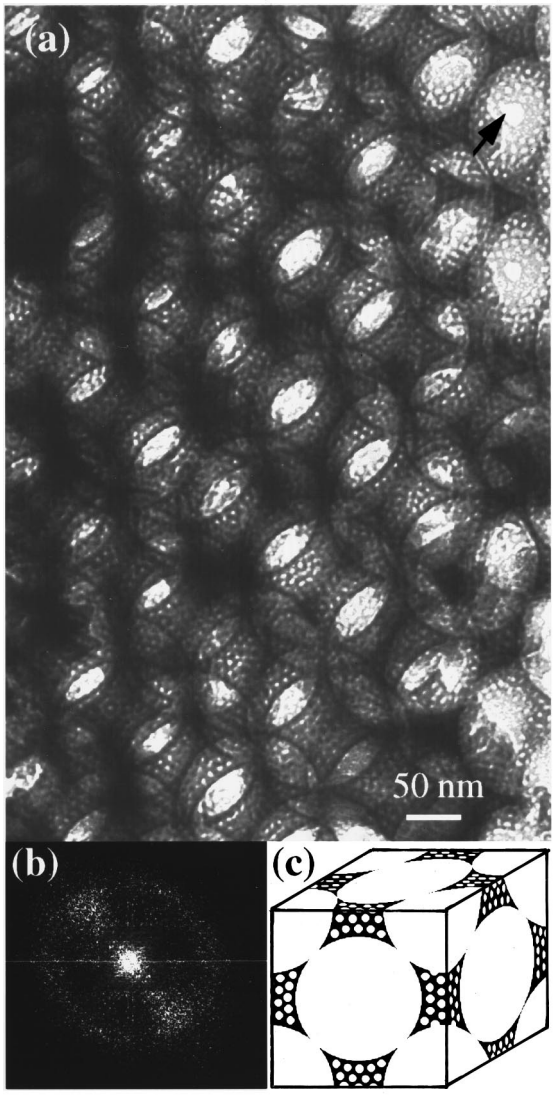

FIG. 1. (a) Transmission electron microscopy image of porous silica, exhibiting ordering in two length scales: close-packed hollow spheres (~120 nm) and self-organized nanocavities (4–5 nm). The arrowhead indicates a hole that interconnects the hollow spheres; (b) Fourier transform of the image confirms the ordering at hollow sphere length scale, while the ordering at nanocavity length scale is not perfect because of the space limitation between the spheres; (c) schematic model of the ordered double length-scale porous nanostructure.

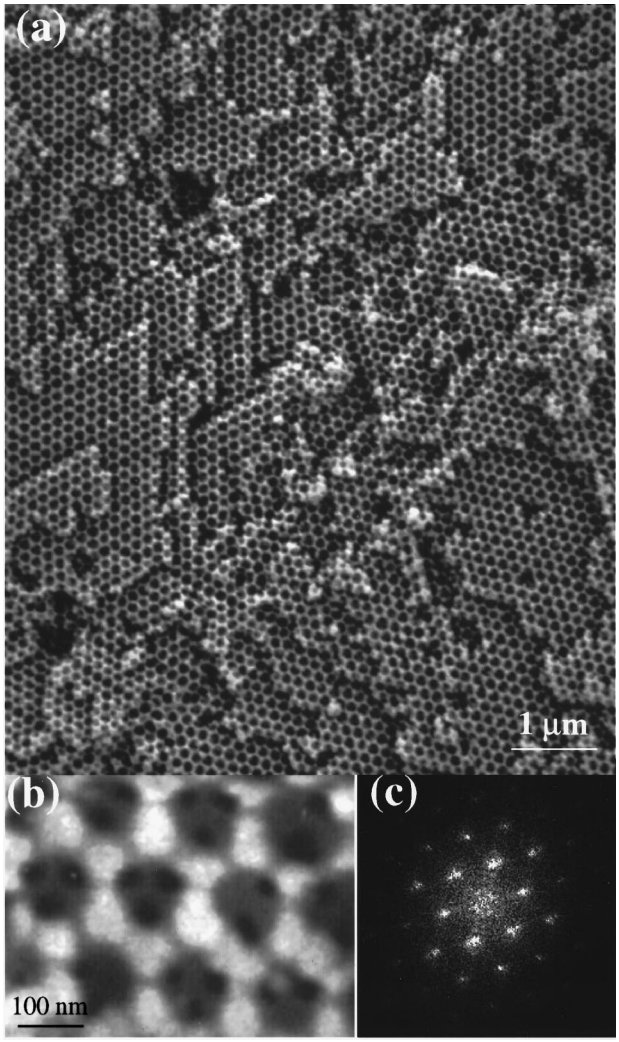

FIG. 2. (a) Scanning electron microscope (SEM) image of the closely packed hollow spheres. The sample was coated with Pt and the image was recorded at 5 kV to minimize charging effect. (b) An enlarged area showing the interior structure of the hollow spheres, where the interconnecting holes between adjacent hollow spheres are displayed; (c) Fourier transform of the SEM image shows the close-packed {111} plane.

erence to the zero-loss peak. The EELS data was acquired at low magnification (×10 000) in the imaging mode at a doweling time of 0.1 s for 20 dowels. Shown in Fig. 3(a) is a comparison of the low-loss EELS spectra recorded from solid silica spheres, mesoporous silica [see Fig. 3(b)] and the DLSO porous silica. The spectra shapes may vary for different materials due to the excitation of surface plasmons and the multiple scattering effect. The plasmon energy shifts from 23.4±0.2 eV for the solid sphere to 22.0±0.2 eV for the mesoporous silica and to 22.4±0.2 eV for the DLSO porous silica. The plasmon energy was measured in reference to the maximum intensity of the peak with consideration of the symmetry of the intensity profile around the peak maximum. The energy shift was observed consistently in the EELS spectra acquired from thin and thick specimen regions and it is not the result of the enhanced surface excitation. The plasmon energies presented here have been examined for specimens with different thicknesses and different data acquisition time, and the data are consistent. The difference in energy shifts between mesoporous and DLSO porous silica is likely associated with the detail of the porous structure. However, no difference was observed in the Si-*L* and O-*K* edges for the three types of specimens.

The volume plasmon is directly related to the dielectric function of the medium. The dielectric function for an insulator material, such as silica, can be qualitatively represented by a harmonic bound-electron model:[10]

$$\epsilon(\omega) \approx 1 + \frac{\omega_p^2}{\omega_n^2 - \omega^2 + i\omega/\tau}$$

$$= 1 + \omega_p^2 \frac{\omega_n^2 - \omega^2}{(\omega_n^2 - \omega^2)^2 + (\omega/\tau)^2}$$

$$+ i\omega_p^2 \frac{\omega/\tau}{(\omega_n^2 - \omega^2)^2 + (\omega/\tau)^2}, \quad (1)$$

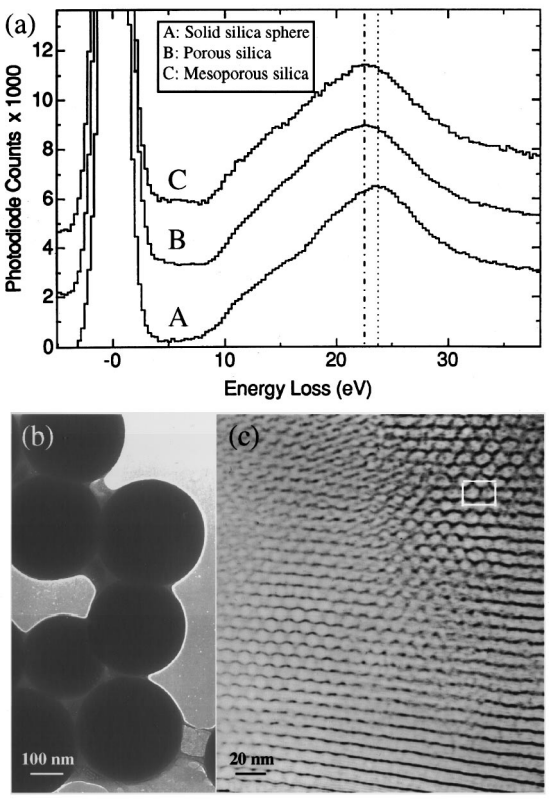

FIG. 3. (a) EELS spectra acquired from (A) solid silica sphere, (b) mesoporous silica, and (C) DLSO porous silica with porosity at double length scale, showing a shift in the volume plasmon energy. The EELS spectra have been deconvoluted with the zero-loss peak to sharpen the resolution. The spectra are displayed by a shift vertically to separate the curves; (b) TEM image of solid silica spheres; (c) TEM image of a mesoporous silica with pore sizes of ~10 nm. The pores are self-organized into a fcc lattice and the [110] projection is shown in the figure.

where $\omega_p=[n_b e^2/\epsilon_0 m]^{1/2}$, n_b is the density of the bound electrons with an eigenfrequency ω_n, m the electron mass, and τ the relaxation time. The resonance frequency of the volume plasmon is determined by $\mathrm{Re}[\epsilon(\omega_v)]=0$.[11] For simplification, the relaxation time τ is assumed to be infinity, thus the plasmon resonance frequency is given by

$$\omega_v=\sqrt{\frac{n_b e^2}{\epsilon_0 m}+\omega_n^2}. \tag{2}$$

The eigenfrequency ω_n is related to the spring constant k, characterizing the bounding force from the nucleus on the electron, by $\omega_n=(k/m)^{1/2}$. Since ω_n is determined by the atomic length-scale structure and it is unlikely to change with the porosity, the observed decrease in ω_v for the porous silica suggests that the local density of the bound electrons drops as a result of the porous structure.

It is known that EELS can be applied to retrieve the dielectric function of a material based on the Kramers–Kronig transformation.[12] This is possible if the surface plasmon excitation is rather small so that the energy-loss function $\mathrm{Im}[-1/\epsilon(\omega)]$ can be attained directly from EELS spectra. For the porous materials, the large surface area results in a dramatic increase in surface plasmon excitation. On the other hand, the spectrum shape of the surface plasmon sensitively depends on the geometry of the scattering object and the impact position of the incident electron.[11] It is nontrivial to derive the energy-loss function from the EELS spectrum for the porous materials described here.

In conclusion, mesoporous nanostructured silica has been prepared using a simple technique, which gives ordering at double length scales. A comparison is given on the low-loss EELS spectra recorded from solid silica spheres, mesoporous silica, and DLSO porous silica. The plasmon energy of the porous silica structures shows a significant shift in comparison to that of the bulk, suggesting that the local density of the bound electrons in the porous structures is likely to be lower than that in the bulk. Therefore, the imaginary part of the dielectric function also drops [see Eq. (1)], leading to even lower dielectric loss in addition to that induced by the volume porosity. With consideration of the flexibility of tunable porosity of the silica by changing the sizes of the template PS spheres and the chain length of the copolymer, this study provides a technique for tuning the electronic structure of silica by varying its porosity. The porous materials are expected to have not only a large surface area for catalysis, but also a low dielectric constant for high-frequency microelectronics. Research is undertaken in these directions.

The authors would like to thank NSF DMR-9733160 for financial support, and Dr. Yongbao Xin for assistance in SEM operation.

[1] O. D. Velev, T. A. Jede, R. F. Lobo, and A. M. Lenhoff, Nature (London) **389**, 448 (1997).
[2] A. Z. Zakhidov, R. H. Baughman, Z. Iqbal, C. Cui, I. Khayrullin, S. O. Dantas, J. Marti, and V. G. Ralchenko, Science **282**, 897 (1998).
[3] J. E. G. J. Wijnhoven and W. L. Vos, Science **281**, 802 (1998).
[4] B. T. Holland, C. F. Blanford, and A. Stein, Science **281**, 538 (1998).
[5] J. D. Joannopoulos, P. R. Villereuue, and S. Fan, Nature (London) **386**, 143 (1997).
[6] C. T. Kresge, M. E. Leonowioz, W. J. Roth, J. C. Vartuli, and J. S. Beck, Nature (London) **359**, 710 (1992).
[7] D. Zhao, J. Feng, Q. Huo, N. Melosh, G. H. Fredrickson, B. F. Chmelka, and G. D. Stucky, Science **279**, 548 (1998).
[8] J. S. Yin and Z. L. Wang, Adv. Mater. (in press).
[9] N. Stöber, A. Fink, and E. Bohn, J. Colloid Interface Sci. **26**, 62 (1968).
[10] H. Raether, *Excitation of Plasmons and Interband Transitions by Electrons* (Springer, New York, 1980), p. 14.
[11] Z. L. Wang, Micron **27**, 265 (1996); **28**, 505 (1997).
[12] Y. Y. Wang, H. Zhang, and V. P. Dravid, Ultramicroscopy **52**, 523 (1993).